

Fibroblastic reticular cells predict response to cancer immunotherapy

Daniele Biasci^{1,2,✉}, James Thaventhiran^{1,2,*}, and Simon Tavaré^{2,3,*}

¹MRC Toxicology Unit, University of Cambridge, Robinson Way, Cambridge, CB2 0RE, United Kingdom

²Cancer Research UK Cambridge Institute, Robinson Way, Cambridge CB2 0RE, United Kingdom

³Herbert and Florence Irving Institute for Cancer Dynamics, Columbia University, Schermerhorn Hall, Suite 601, 1190 Amsterdam Ave, New York, NY 10027, United States

1 While the role of CD8+ T cells in mediating response to cancer
2 immunotherapy is well established, the role of other cell types,
3 including B cells, remains more controversial. By conducting
4 the largest gene expression study of response to immune check-
5 point blockade (ICB) to date, here we show that pre-treatment
6 expression of B cell genes is associated with ICB response inde-
7 pendently of CD8+ T cells. Strikingly, we discovered that such
8 association is completely explained by a single gene expressed
9 in fibroblastic reticular cells (FRCs). We further validated this
10 finding in three independent cohorts of patients treated with
11 ICB, in both melanoma and renal cell carcinoma.

12 The role of B cells in cancer immunotherapy is currently a
13 matter of debate (1–3). Recently, it has been reported that
14 expression of B cell specific genes inside tumours is asso-
15 ciated with response to immune checkpoint blockade (ICB),
16 thus suggesting an unappreciated biological role for B cells in
17 promoting ICB response (4). However, association between
18 B cell gene expression and ICB response was not statisti-
19 cally significant when other immune populations, including
20 CD8+ T cells, were taken into account (4). For this rea-
21 son, it remains unclear whether B cells are associated with
22 ICB response independently of CD8+ T cells. Clarifying this
23 point is crucial for the biological interpretation of these re-
24 sults. In fact, expression of B cell specific genes in the tu-
25 mour microenvironment (TME) is often strongly correlated
26 with markers of CD8+ T cells (5), which express the ac-
27 tual molecular targets of ICB treatment and are a validated
28 predictor of immunotherapy response (6–8). Two additional
29 recent studies on this topic did not address the issue, be-
30 cause they described predictive signatures containing both B
31 cell and CD8+ T cell markers, as well as genes expressed
32 in other immune cell types (9, 10). In order to address this
33 problem, we analysed the entire transcriptome of a larger
34 number of melanoma samples compared to previous studies
35 ($n = 366$), and we then considered only samples collected
36 before commencing treatment with immune checkpoint in-
37 hibitors. Moreover, we excluded tumour samples obtained
38 from lymph node metastasis, in order to minimise the risk
39 of capturing unrelated immune populations from the adja-
40 cent lymphoid tissue (see supplementary methods). We cal-
41 culated the correlation between expression of each gene at
42 baseline and subsequent treatment response, as defined in the
43 original studies according to the RECIST criteria (11). A
44 distinct group of genes showed significant association with

45 treatment response, namely: *CR2* (CD21), *MS4A1* (CD20),
46 *CD19*, *FCER2* (CD23), *PAX5*, *BANK1*, *VPREB3*, *TCLIA*,
47 *CLEC17A* and *FDCSP* (Fig. 1A and Table S1). Literature
48 reports that these genes are predominantly expressed in B
49 cells (12), with the exception of *FDCSP*, which was found to
50 be expressed follicular dendritic cells (FDCs) isolated from
51 secondary lymphoid organs, but not in B cells (13, 14). In
52 order to identify the cell populations expressing these genes
53 in tumours, we assessed their expression in single-cell RNA
54 sequencing data (scRNAseq) from human cancer samples
55 (15). First, we confirmed that genes identified by our associ-
56 ation study were specifically expressed in tumour-associated
57 B cells (Fig. S8). Second, we observed that *FDCSP* was not
58 expressed in tumour-associated B cells (Fig. S1), but identi-
59 fied a subset of fibroblastic cells (*FAP+* *COL1A1+* *CD31-*
60 ; Fig. S2) expressing markers consistent with FRC iden-
61 tity (*CCL19+* *CCL21+* *BAFF+*; 16, 17; Figures S3 and S4
62 and tables S5 and S6). Finally, we confirmed these results
63 in an independent set of melanoma samples profiled at the
64 single-cell level (18; Figures S4 to S7 and S9). We then
65 sought to determine whether expression of these genes was
66 associated with ICB response independently of CD8+ T cell
67 infiltration. To this aim, we repeated the association anal-
68 ysis after taking into account expression markers of T cells,
69 NK cells, cross-presenting dendritic cells (19) and interferon-
70 gamma response (20; Fig. 1D and table S1). We found that
71 only four genes were associated with ICB response indepen-
72 dently of all immune markers considered: *MS4A1* (prototyp-
73 ical B cell marker), *CLEC17A* (expressed in dividing B cells
74 in germinal centers; 21), *CR2* (expressed in mature B cells
75 and FDCs; 22) and *FDCSP* (expressed in FRCs but not in
76 B cells). This result suggested that presence of B cells and
77 FRCs in the tumour microenvironment (TME) before treat-
78 ment was associated with subsequent ICB response indepen-
79 dently of CD8+ T cells (Fig. 1D and Table S7). Remark-
80 ably, we observed that *FDCSP* remained significantly associ-
81 ated with ICB response even after B cell markers were taken
82 into account (Fig. 1D) and that no other gene remained sig-
83 nificant after *FDCSP* expression was included in the model
84 (Fig. 1D). Taken together, these results suggest that expres-
85 sion of *FDCSP* might be an independent predictor of ICB
86 response. We tested this hypothesis in a completely inde-
87 pendent cohort of melanoma patients treated with anti-PD1,
88 either alone or in combination with anti-CTLA4 (23). In this
89 validation cohort, patients with higher expression of *FDCSP*
90 at baseline experienced significantly longer overall survival

* These authors have contributed equally to this work.

(log-rank $p < 0.0001$) and progression-free survival (log-rank $p < 0.0001$) after commencing treatment with ICB (Figures 1B and 1C). Moreover, we observed a significant association between expression of *FDCSP* at baseline and subsequent RECIST response (Cochran-Armitage test $p < 0.0001$; Fig. 1E). We sought to replicate this observation in two additional independent cohorts of patients treated with ICB in melanoma (4) and clear cell renal cell carcinoma (24) and found similar results (Figures 1F and 1G). On the other hand, testing B cell markers in the validation cohorts produced less consistent results (Fig. S10). Finally, we performed multiple linear regression analysis and found that the association between *FDCSP* and ICB response was independent of CD8+ T cells, CD4+ T cells, B cells, NK cells, myeloid Dendritic cells (mDCs), Macrophages and Plasma cells (Tables S2 and S3). While CD8+ T cells express the molecular targets of ICB, and their presence in the TME is a validated predictor of ICB response (6–8), the role of B cells remains more controversial (1–3). Because T and B cells often co-occur in the TME (25), gene expression studies consistently reported strong correlation between T cells, B cells and other immune cell types, especially in melanoma (5). As a consequence, assessing whether B cells are associated with ICB response independently of CD8+ T cells has been proven challenging (4). By analysing a larger number of samples compared to previous studies, we were able to demonstrate that B cells predict ICB response independently of CD8+ T cells (Fig. 1D and Table S4). This supports the idea that B cells might actively promote ICB response (3), rather than being irrelevant (2) or detrimental to it (1). However, our data also shows that such positive association can be completely explained by a single gene expressed outside of the B cell compartment. We have demonstrated that *FDCSP* is transcribed in a subset of fibroblastic cells up-regulating *CCL19*, *CCL21* and *BAFF* and down-regulating genes associated with canonical fibroblasts, such as extracellular matrix genes (Fig. S4, Table S5, Table S6), an expression pattern consistent with FRC identity (16, 17). One way to reconcile these observations is to consider that FRCs are required to initiate efficient B and T cell responses (16). In both secondary lymphoid organs (SLO) and tertiary lymphoid structures (TLS), FRCs form reticular networks that facilitate interactions between B cells, T cells and their cognate antigens (17, 26). Homing of immune cells into the network requires interaction between chemokines produced by FRCs (*CCL19* and *CCL21*) and their receptor (*CCR7*) expressed on T cells, B cells and dendritic cells (27, 28; see also Table S1). Accordingly, depleting FRCs causes loss of T cells, B cells and dendritic cells in both SLO and TLS and decreases the magnitude of B and T cell responses to subsequent viral infection (16, 29). Perhaps more importantly, differentiation of fibroblasts into FRCs occurs early during TLS formation, precedes B and T cell infiltration and can still be observed in *Rag2*^{-/-} mice (29). In this context, our finding that a gene expressed in FRCs is associated with ICB response independently of B and T cell infiltration is coherent with the current understanding of TLS neogenesis. Taken together, these observa-

tions suggest that the reported association between B cells and ICB response (4), albeit independent of CD8+ T cells, might ultimately be secondary to the presence of FRCs in the TME. The identification of *FDCSP* as a single marker of ICB response should enable even larger studies to test this conclusion. To our knowledge, this is the first time that FRCs are directly implicated in ICB response, thus opening new avenues to explain why some patients do not respond to cancer immunotherapy.

Bibliography

1. Somasundaram, R. *et al.* Tumor-associated b-cells induce tumor heterogeneity and therapy resistance. *Nature communications* **8**, 1–16 (2017).
2. Damsky, W. *et al.* B cell depletion or absence does not impede anti-tumor activity of pd-1 inhibitors. *Journal for immunotherapy of cancer* **7**, 153 (2019).
3. Hollern, D. P. *et al.* B cells and t follicular helper cells mediate response to checkpoint inhibitors in high mutation burden mouse models of breast cancer. *Cell* **179**, 1191–1206 (2019).
4. Helmink, B. A. *et al.* B cells and tertiary lymphoid structures promote immunotherapy response. *Nature* (2020).
5. Iglesia, M. D. *et al.* Genomic analysis of immune cell infiltrates across 11 tumor types. *JNCI: Journal of the National Cancer Institute* **108** (2016).
6. Ji, R.-R. *et al.* An immune-active tumor microenvironment favors clinical response to ipilimumab. *Cancer Immunology, Immunotherapy* **61**, 1019–1031 (2012).
7. Ayers, M. *et al.* Ifn- γ -related mrna profile predicts clinical response to pd-1 blockade. *The Journal of clinical investigation* **127**, 2930–2940 (2017).
8. Cristescu, R. *et al.* Pan-tumor genomic biomarkers for pd-1 checkpoint blockade-based immunotherapy. *Science* **362**, eaar3593 (2018).
9. Cabrita, R. *et al.* Tertiary lymphoid structures improve immunotherapy and survival in melanoma. *Nature* (2020).
10. Petitprez, F. *et al.* B cells are associated with survival and immunotherapy response in sarcoma. *Nature* (2020).
11. Schwartz, L. H. *et al.* Recist 1.1—update and clarification: From the recist committee. *European journal of cancer* **62**, 132–137 (2016).
12. Kassambara, A. *et al.* Genomicscape: an easy-to-use web tool for gene expression data analysis. application to investigate the molecular events in the differentiation of b cells into plasma cells. *PLoS computational biology* **11**, e1004077 (2015).
13. Marshall, A. J. *et al.* Fdc-sp, a novel secreted protein expressed by follicular dendritic cells. *The Journal of Immunology* **169**, 2381–2389 (2002).
14. Al-Alwan, M. *et al.* Follicular dendritic cell secreted protein (fdc-sp) regulates germinal center and antibody responses. *The Journal of Immunology* **178**, 7859–7867 (2007).
15. Zilionis, R. *et al.* Single-cell transcriptomics of human and mouse lung cancers reveals conserved myeloid populations across individuals and species. *Immunity* **50**, 1317–1334 (2019).
16. Denton, A. E., Roberts, E. W., Linterman, M. A. & Fearon, D. T. Fibroblastic reticular cells of the lymph node are required for retention of resting but not activated cd8+ t cells. *Proceedings of the National Academy of Sciences* **111**, 12139–12144 (2014).
17. Cremasco, V. *et al.* B cell homeostasis and follicle confinement are governed by fibroblastic reticular cells. *Nature immunology* **15**, 973–981 (2014).
18. Jerby-Aron, L. *et al.* A cancer cell program promotes t cell exclusion and resistance to checkpoint blockade. *Cell* **175**, 984–997 (2018).
19. Hartung, E. *et al.* Induction of potent CD8 t cell cytotoxicity by specific targeting of antigen to cross-presenting dendritic cells in vivo via murine or human XCR1. *The Journal of Immunology* **194**, 1069–1079 (2014).
20. Chow, M. T. *et al.* Intratumoral activity of the cxcr3 chemokine system is required for the efficacy of anti-pd-1 therapy. *Immunity* **50**, 1498–1512 (2019).
21. Graham, S. A. *et al.* Prolectin, a glycan-binding receptor on dividing b cells in germinal centers. *Journal of Biological Chemistry* **284**, 18537–18544 (2009).
22. Takahashi, K. *et al.* Mouse complement receptors type 1 (cr1; cd35) and type 2 (cr2; cd21): expression on normal b cell subpopulations and decreased levels during the development of autoimmunity in mrl/lpr mice. *The Journal of Immunology* **159**, 1557–1569 (1997).
23. Gide, T. N. *et al.* Distinct immune cell populations define response to anti-pd-1 monotherapy and anti-pd-1/anti-ctla-4 combined therapy. *Cancer cell* **35**, 238–255 (2019).
24. Miao, D. *et al.* Genomic correlates of response to immune checkpoint therapies in clear cell renal cell carcinoma. *Science* **359**, 801–806 (2018).
25. Garnelo, M. *et al.* Interaction between tumour-infiltrating b cells and t cells controls the progression of hepatocellular carcinoma. *Gut* **66**, 342–351 (2017).
26. Denton, A. E., Carr, E. J., Magiera, L. P., Watts, A. J. & Fearon, D. T. Embryonic fap- lymphoid tissue organizer cells generate the reticular network of adult lymph nodes. *Journal of Experimental Medicine* **216**, 2242–2252 (2019).
27. Gunn, M. D. *et al.* Mice lacking expression of secondary lymphoid organ chemokine have defects in lymphocyte homing and dendritic cell localization. *The Journal of experimental medicine* **189**, 451–460 (1999).
28. Förster, R. *et al.* *Ccr7* coordinates the primary immune response by establishing functional microenvironments in secondary lymphoid organs. *Cell* **99**, 23–33 (1999).
29. Nayar, S. *et al.* Immunofibroblasts are pivotal drivers of tertiary lymphoid structure formation and local pathology. *Proceedings of the National Academy of Sciences* **116**, 13490–13497 (2019).

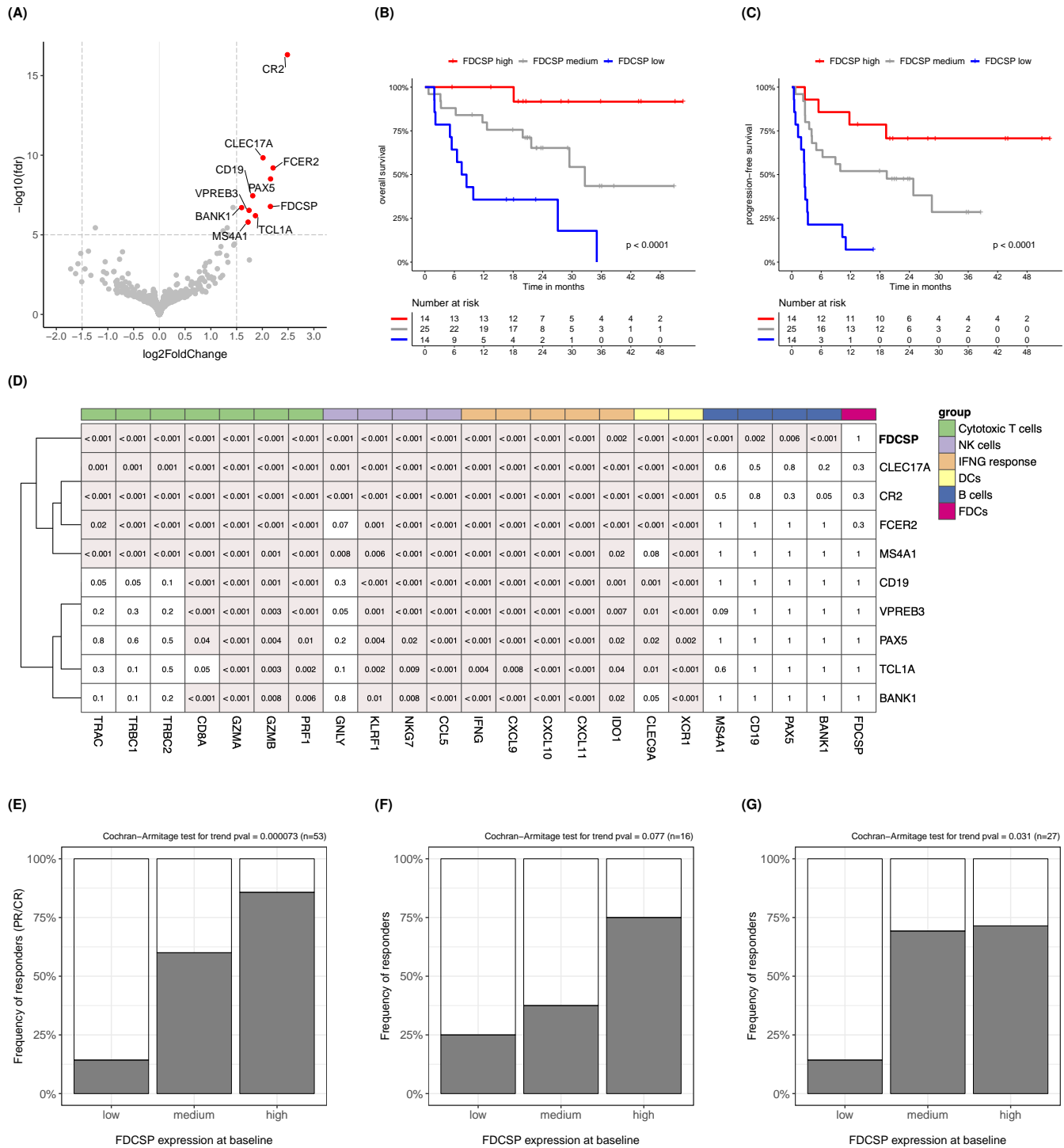


Fig. 1. | Expression of FDCSP is an independent predictor of response to immune checkpoint blockade. **A.** Volcano plot showing genes significantly associated with response to ICB. **B-C** Kaplan-Meier curves showing different overall survival and progression-free survival in melanoma patients after commencing treatment with ICB. Patients from the first validation cohort (23; see supplementary methods) were stratified in three groups according to pre-treatment expression of *FDCSP*. **D** Heatmap showing association between pre-treatment expression of B cell or FRC genes (rows) and subsequent ICB response after the effect of other immune markers (columns) was taken into account. The number inside each cell represents the Wald test p-value for the underlying effect size estimate obtained using the negative binomial model for RNAseq counts implemented in DESeq2 (see supplementary methods). Nominal p-values were corrected for multiple testing using Benjamini-Yekutieli false discovery rate (FDR) and are also reported in Table S7. A red background highlights effect sizes estimated to be greater than zero with FDR < 0.05. In this study, an effect size greater than zero represents a positive association between gene expression and probability of ICB response. **E-G** Association between pre-treatment expression of *FDCSP* and subsequent ICB response in the first (23), second (4) and third validation cohort (24). See supplementary methods.

225 Appendix S1: supplementary methods

226 **Bulk RNAseq: discovery cohorts.** The RNAseq datasets used in this study as discovery cohorts were downloaded from
227 the following published sources: data for 27 melanoma samples from patients that went on to receive ICB treatment was
228 downloaded from the NIH Genomics Data Common Portal, study TCGA-SKCM (1, 2); data for 42 pre-ICB melanoma samples
229 was downloaded from dbGaP (3), study phs000452.v2.p1 (4); data for 109 melanoma samples collected before or during ICB
230 treatment was downloaded from Gene Expression Omnibus (GEO; 5), series GSE91061 (6); data for 28 melanoma samples
231 collected before ICB treatment was downloaded from GEO, series GSE78220 (7); data for 37 melanoma samples collected
232 before or during ICB treatment was downloaded from GEO, series GSE115821 (8). Clinical annotations for each sample
233 (i.e. type of ICB treatment received, sample collection time point, tumour site, treatment response) were obtained from the
234 original publications. Samples collected after commencing treatment with ICB, samples obtained from lymph node metastasis,
235 and samples for which treatment response status was not available were excluded from subsequent analyses, leaving 137 pre-
236 treatment samples available for this study.

237 **Bulk RNAseq: validation cohorts.** The RNAseq datasets used in this study as validation cohorts were downloaded from the
238 following published sources. *First validation cohort:* data for 91 melanoma samples collected before or during ICB treatment
239 was downloaded from the European Nucleotide Archive (ENA; 9), study PRJEB23709 (10). *Second validation cohort:* data
240 for 16 melanoma samples collected before ICB treatment was obtained from (11). *Third validation cohort:* data for 33 clear
241 cell renal cell carcinoma samples collected before ICB treatment was obtained from (12). Clinical annotations for each sample
242 were obtained from the original publications. Samples collected after commencing treatment with ICB and samples for which
243 treatment response status was not available were excluded from subsequent analyses.

244 **Bulk RNAseq: gene expression quantification.** Sequences of all known human transcripts were downloaded from Ensembl
245 release 97 (13). Transcript quantification was performed using Kallisto ver. 0.43 (14) and gene-level count matrices for use in
246 DESeq2 (15) were calculated using tximport (16) as recommended by DESeq2 authors (17). All subsequent analyses on gene
247 expression were performed using R 3.5.0 (18). For differential expression analysis, raw counts were used directly in DESeq2 as
248 recommended (17). For other downstream analyses (i.e. survival curves, multiple correlation analysis and others) counts data
249 were transformed using the variance stabilizing transformation (19) as implemented in DESeq2 (17) and potential systematic
250 differences between cohorts were corrected using ComBat (20) as implemented in the sva package (21). The methods described
251 in this section were used to quantify gene expression in all datasets used in this study as discovery cohorts and for the first
252 validation cohort, for which original FASTQ files were available. For the second and third validation cohort (10), we used the
253 gene expression values provided in the original publications (11, 12).

254 **Bulk RNAseq: genes associated with ICB response.** In the discovery cohorts, association between gene expression and
255 ICB response was calculated using the DESeq2 model based on the negative binomial distribution (15). Raw counts for each
256 gene were used directly in the model as recommended by DESeq2 authors (17). We used the ICB response status for each
257 patient as reported in the original study (1, 4, 6–8) according to the RECIST criteria (22). RECIST response categories were
258 encoded as a numerical score as follows: PD (progressive disease) = -1, SD (stable disease) = 0, PR (partial response) = 0.5,
259 CR (complete response) = 1. When we assessed the use of a different numerical score (i.e. PD = 0, SD = 0.33, PR = 0.66,
260 CR = 1), we obtained similar results. In order to account for systematic differences between cohorts, a categorical variable
261 encoding the cohort of origin for each sample was included as a covariate in the DESeq2 association model. In order to take
262 into account the effect of known immune markers (Fig. 1D), the association analysis was repeated after their expression level
263 was calculated according to DESeq2 documentation (17) and added to the model as an additional covariate.

264 **Bulk RNAseq: survival curves.** Survival curves were plotted using the R package survminer (23). Patients were stratified in
265 three groups according to the baseline expression of the gene of interest: the high expression group was defined as containing
266 the 25% of samples with highest expression, the low expression group was defined as containing the 25% of samples with
267 lowest expression, and the medium expression group was defined as containing the remaining samples. Statistical significance
268 of the observed difference between groups was assessed using the Logrank test (24).

269 **Single-cell RNAseq: original data sets.** Expression values (normalised counts) for 54773 single cells isolated from non-
270 small-cell lung cancer (NSCLC) tumour samples were downloaded from GEO, series GSE127465 (25). Cell type annotation
271 and a two-dimensional visualisation (SPRING plot, 26) of single-cell transcriptomes were also obtained from the original pub-
272 lication (25) and used for subsequent analyses. Expression values (transcripts per million) for 7186 single cells isolated from
273 melanoma samples were downloaded from GEO, series GSE115978 (27). Cell type annotation and a two-dimensional visual-
274 isation (tSNE plot, 28) of single-cell transcriptomes were obtained from the original publication (27) and used for subsequent
275 analyses.

276 **Single-cell RNAseq: differentially expressed genes.** Expression values obtained from GSE127465 and GSE115978 were
277 transformed in logarithmic scale ($y = \log_2(x + 1)$). Cells annotated as fibroblasts in the original study were selected and
278 used to compare fibroblasts expressing *FDCSP* (*FDCSP+*) against fibroblasts not expressing *FDCSP* (*FDCSP-*). Statistical
279 significance for gene expression differences observed between these two groups was assessed using unpaired two-samples
280 Wilcoxon test (29). Genes were ranked using a numerical score which takes into account both p-value and $\log_2(fc)$: score
281 $= \sqrt{-\log_{10}(p - \text{value})} * |\log_2(fc)| * \text{sign}(\log_2(fc))$. Results for GSE127465 (non-small cell lung cancer) and GSE115978
282 (melanoma) were meta-analysed using the RankProduct method (30, 31) and are presented in Tables S5 and S6.

283 **Code availability.** The authors declare that the code used for this study is available upon request.

284 Supplementary methods references.

- 285 1. Akbani, R. *et al.* Genomic classification of cutaneous melanoma. *Cell* **161**, 1681–1696 (2015).
- 286 2. Grossman, R. L. *et al.* Toward a shared vision for cancer genomic data. *New England Journal of Medicine* **375**, 1109–1112 (2016).
- 287 3. Mailman, M. D. *et al.* The ncbi dbgap database of genotypes and phenotypes. *Nature genetics* **39**, 1181–1186 (2007).
- 288 4. Van Allen, E. M. *et al.* Genomic correlates of response to ctla-4 blockade in metastatic melanoma. *Science* **350**, 207–211 (2015).
- 289 5. Edgar, R., Domrachev, M. & Lash, A. E. Gene expression omnibus: Ncbi gene expression and hybridization array data repository. *Nucleic acids research* **30**, 207–210 (2002).
- 290 6. Riaz, N. *et al.* Tumor and microenvironment evolution during immunotherapy with nivolumab. *Cell* **171**, 934–949 (2017).
- 291 7. Hugo, W. *et al.* Genomic and transcriptomic features of response to anti-pd-1 therapy in metastatic melanoma. *Cell* **165**, 35–44 (2016).
- 292 8. Auslander, N. *et al.* Robust prediction of response to immune checkpoint blockade therapy in metastatic melanoma. *Nature medicine* **24**, 1545–1549 (2018).
- 293 9. Leinonen, R. *et al.* The european nucleotide archive. *Nucleic acids research* **39**, D28–D31 (2010).
- 294 10. Gide, T. N. *et al.* Distinct immune cell populations define response to anti-pd-1 monotherapy and anti-pd-1/anti-ctla-4 combined therapy. *Cancer cell* **35**, 238–255 (2019).
- 295 11. Helmkink, B. A. *et al.* B cells and tertiary lymphoid structures promote immunotherapy response. *Nature* (2020).
- 296 12. Miao, D. *et al.* Genomic correlates of response to immune checkpoint therapies in clear cell renal cell carcinoma. *Science* **359**, 801–806 (2018).
- 297 13. Cunningham, F. *et al.* Ensembl 2019. *Nucleic Acids Research* **47**, D745–D751 (2018). URL <https://doi.org/10.1093/nar/gky1113>.
- 298 14. Bray, N. L., Pimentel, H., Melsted, P. & Pachter, L. Near-optimal probabilistic RNA-seq quantification. *Nature Biotechnology* **34**, 525–527 (2016). URL <https://doi.org/10.1038/nbt.3519>.
- 299 15. Love, M. I., Huber, W. & Anders, S. Moderated estimation of fold change and dispersion for RNA-seq data with DESeq2. *Genome Biology* **15** (2014). URL <https://doi.org/10.1186/s13059-014-0550-8>.
- 300 16. Soneson, C., Love, M. I. & Robinson, M. D. Differential analyses for RNA-seq: transcript-level estimates improve gene-level inferences. *F1000Research* **4**, 1521 (2015). URL <https://doi.org/10.12688/f1000research.7563.1>.
- 301 17. Love, M. I., Anders, S. & Huber, W. Analyzing rna-seq data with deseq2 (2019). URL <http://bioconductor.org/packages/devel/bioc/vignettes/DESeq2/inst/doc/DESeq2.html#tximport>.
- 302 18. R Core Team. *R: A Language and Environment for Statistical Computing*. R Foundation for Statistical Computing, Vienna, Austria (2018). URL <https://www.R-project.org/>.
- 303 19. Huber, W., von Heydebreck, A., Sultmann, H., Poustka, A. & Vingron, M. Parameter estimation for the calibration and variance stabilization of microarray data. *Statistical applications in genetics and molecular biology* **2** (2003).
- 304 20. Johnson, W. E., Li, C. & Rabinovic, A. Adjusting batch effects in microarray expression data using empirical bayes methods. *Biostatistics* **8**, 118–127 (2007).
- 305 21. Leek, J. T. *et al.* Sva: surrogate variable analysis. 2015. *R package version 3*, 25–27.
- 306 22. Schwartz, L. H. *et al.* Recist 1.1—update and clarification: From the recist committee. *European journal of cancer* **62**, 132–137 (2016).
- 307 23. Kassambara, A., Kosinski, M., Biecek, P. & Fabian, S. Package 'survminer'. *Drawing Survival Curves using 'ggplot2'*. (R package version 0.3. 1.) (2017).
- 308 24. Peto, R. & Peto, J. Asymptotically efficient rank invariant test procedures. *Journal of the Royal Statistical Society: Series A (General)* **135**, 185–198 (1972).
- 309 25. Zilionis, R. *et al.* Single-cell transcriptomics of human and mouse lung cancers reveals conserved myeloid populations across individuals and species. *Immunity* **50**, 1317–1334 (2019).
- 310 26. Weinreb, C., Wolock, S. & Klein, A. M. Spring: a kinetic interface for visualizing high dimensional single-cell expression data. *Bioinformatics* **34**, 1246–1248 (2018).
- 311 27. Jerby-Arnon, L. *et al.* A cancer cell program promotes t cell exclusion and resistance to checkpoint blockade. *Cell* **175**, 984–997 (2018).
- 312 28. Maaten, L. v. d. & Hinton, G. Visualizing data using t-sne. *Journal of machine learning research* **9**, 2579–2605 (2008).
- 313 29. Mann, H. B. & Whitney, D. R. On a test of whether one of two random variables is stochastically larger than the other. *The annals of mathematical statistics* 50–60 (1947).
- 314 30. Breitling, R., Armengaud, P., Amtmann, A. & Herzyk, P. Rank products: a simple, yet powerful, new method to detect differentially regulated genes in replicated microarray experiments. *FEBS letters* **573**, 83–92 (2004).
- 315 31. Hong, F. & Breitling, R. A comparison of meta-analysis methods for detecting differentially expressed genes in microarray experiments. *Bioinformatics* **24**, 374–382 (2008).
- 316
- 317
- 318
- 319
- 320

321 **Appendix S2: supplementary figures**

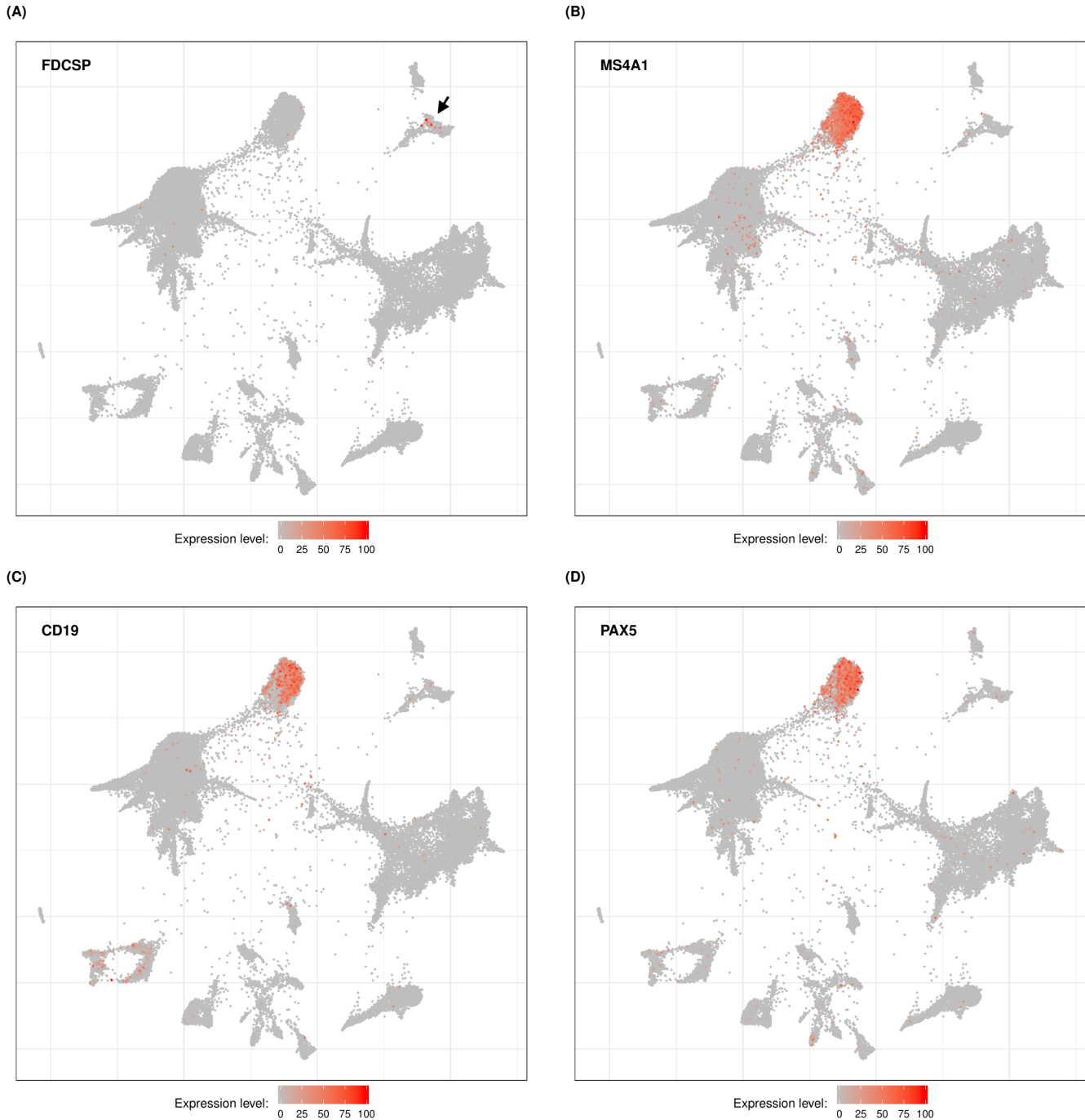


Fig. S1. | FDCSP is not expressed in B cells infiltrating lung cancer tumours. Two-dimensional visualizations (SPRING plots) of single-cell RNA sequencing data obtained from lung cancer tumours and published in (25). Each dot represents the transcriptional profile of a single cell. Cells closely associated in each plot are more likely to transcribe similar genes and might thus belong to the same cell type. Expression values and coordinates for each dot were obtained from the original study. The color scale indicates expression level for a particular gene ranging from 0 (minimum expression value observed in the dataset for that gene, usually corresponding to non detectable expression) to 100 (maximum expression value observed in the dataset for that gene). Expression of *FDCSP* is observed in a group of cells indicated by the black arrow in (A) well distinct from cells expressing prototypical B cell markers (B-D).

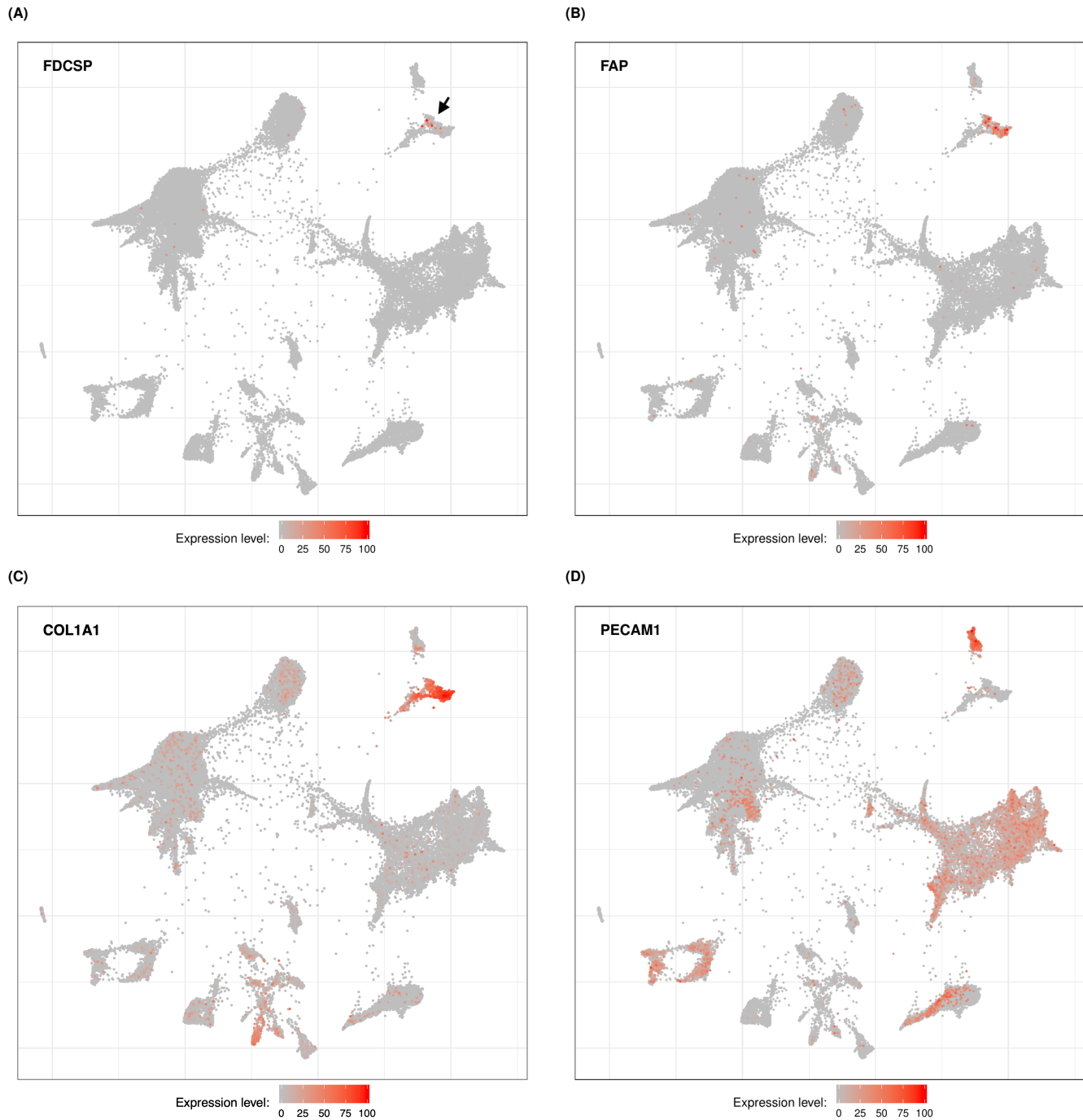


Fig. S2. | FDCSP is expressed in a subset of fibroblasts in lung cancer tumours. Two-dimensional visualizations (SPRING plots) of single-cell RNA sequencing data obtained from lung cancer tumours and published in (25). Each dot represents the transcriptional profile of a single cell. Cells closely associated in each plot are more likely to transcribe similar genes and might thus belong to the same cell type. Expression values and coordinates for each dot were obtained from the original study. The color scale indicates expression level for a particular gene ranging from 0 (minimum expression value observed in the dataset for that gene, usually corresponding to non detectable expression) to 100 (maximum expression value observed in the dataset for that gene). **A.** Expression of *FDCSP*. The black arrow indicates a group of transcriptionally related cells containing *FDCSP*⁺ cells. **B.** Expression of *FAP*. **C.** Expression of *COL1A1*. **D.** Expression of *PECAM1/CD31*.

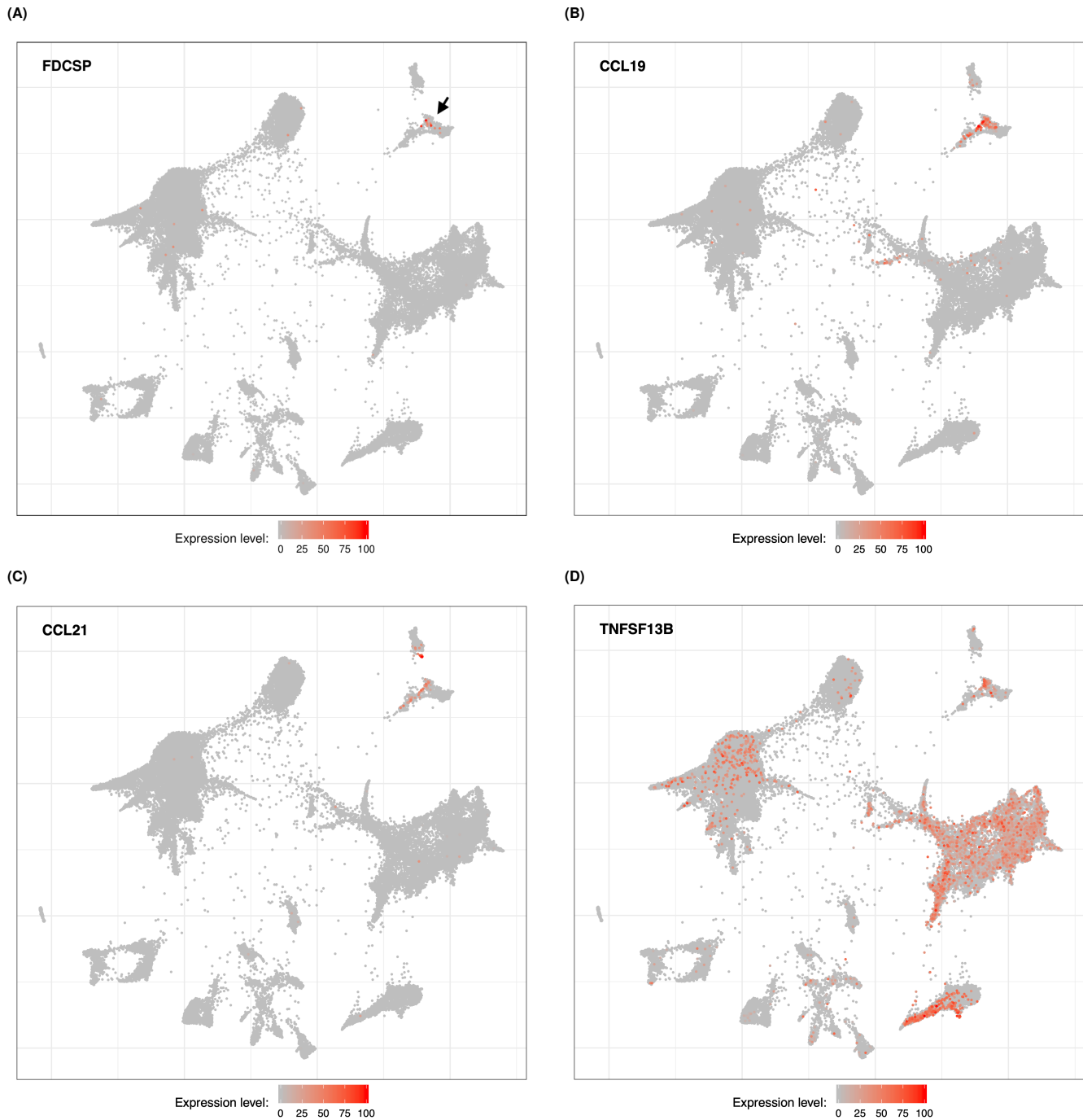


Fig. S3. | FDCSP+ cells express markers of FRCs in lung cancer tumours. Two-dimensional visualizations (SPRING plots) of single-cell RNA sequencing data obtained from lung cancer tumours and published in (25). Each dot represents the transcriptional profile of a single cell. Cells closely associated in each plot are more likely to transcribe similar genes and might thus belong to the same cell type. Expression values and coordinates for each dot were obtained from the original study. The color scale indicates expression level for a particular gene ranging from 0 (minimum expression value observed in the dataset for that gene, usually corresponding to non detectable expression) to 100 (maximum expression value observed in the dataset for that gene). **A.** Expression of *FDCSP*. The black arrow indicates a group of transcriptionally related cells containing *FDCSP*+ cells. **B.** Expression of *CCL19*. **C.** Expression of *CCL21*. **D.** Expression of *TNFSF13B/BAFF*.

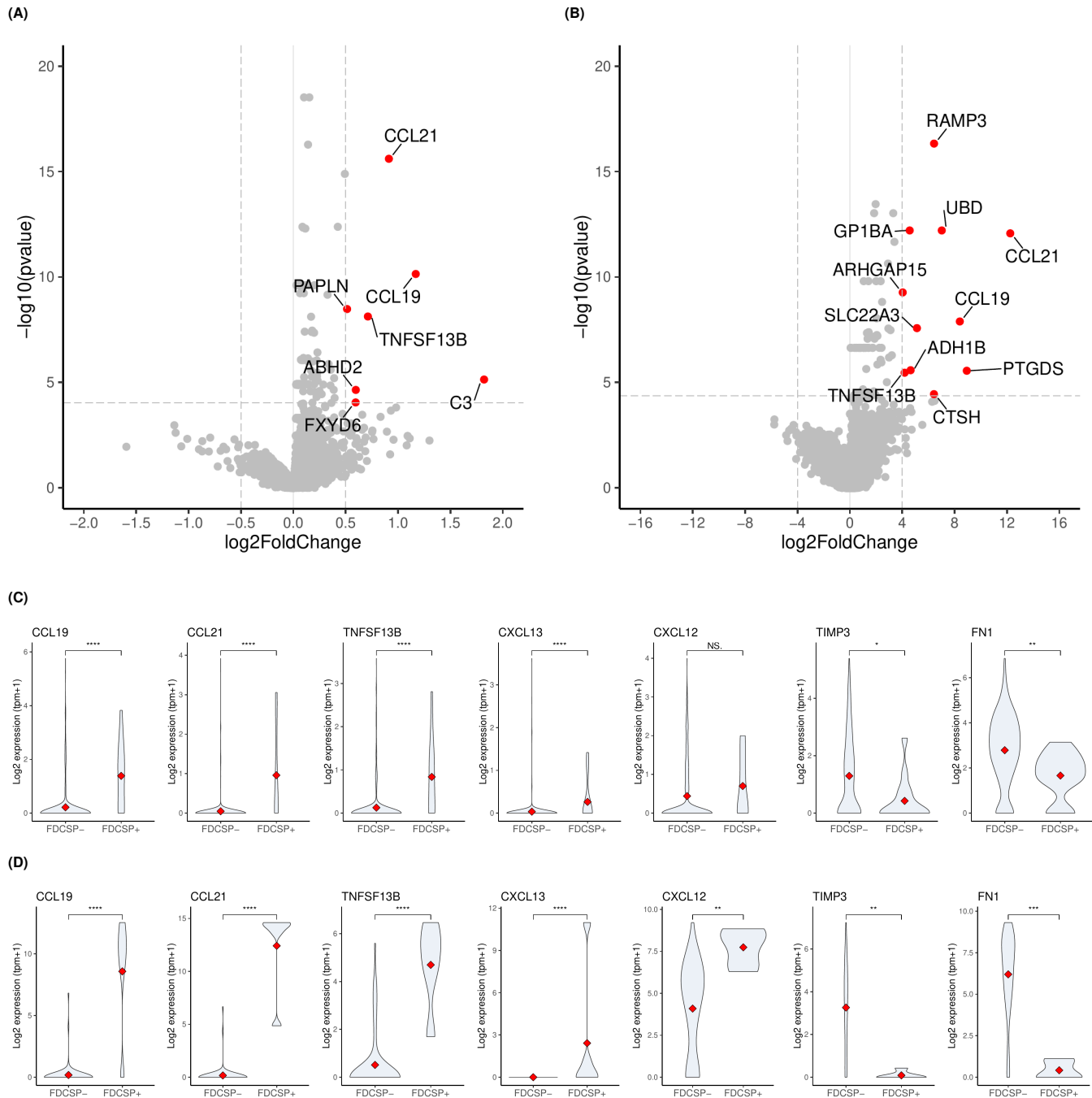


Fig. S4. | *FDCSP+* fibroblasts upregulate FRCs markers in lung cancer and melanoma. Differential gene expression analysis comparing single-cell transcriptomes of *FDCSP+* fibroblasts versus *FDCSP-* fibroblasts obtained from lung cancer and melanoma tumours. The analysis was performed using gene expression data published in (25, 27); see also supplementary methods, Table S5 and Table S6. **A.** Volcano plot representing genes differentially expressed between *FDCSP+* and *FDCSP-* fibroblasts shows that *FDCSP+* fibroblasts significantly upregulate expression of FRCs markers (*CCL19*, *CCL21*, *TNFSF13B/BAFF*) in lung cancer. Genes considered significantly up-regulated ($\log_2(f_c) > \max(\log_2(f_c))/4$ and $\text{FDR} < 0.05$) are marked in red; dotted lines represent chosen $\log_2(f_c)$ and FDR cutoffs. **B.** Volcano plot representing genes differentially expressed between *FDCSP+* and *FDCSP-* fibroblasts and confirming significant up-regulation of FRCs markers in melanoma. **C.** Violin plots comparing distribution of gene expression values in *FDCSP+* and *FDCSP-* fibroblasts in lung cancer. The plots shows that *FDCSP+* fibroblasts significantly upregulate cytokines relevant to FRCs function while down-regulating genes involved in secretion of the extracellular matrix (*TIMP3*, *FN1*). Statistical significance was assessed using unpaired two-samples Wilcoxon test. A red diamond represents the median value of each distribution. **D.** Comparing *FDCSP+* and *FDCSP-* obtained from melanoma tumours leads to similar results (see panel C).



Fig. S5. | FDCSP is not expressed in B cells infiltrating melanoma. Two-dimensional visualizations (tSNE plots) of single-cell RNA sequencing data obtained from melanoma tumours and published in (27). Each dot represents the transcriptional profile of a single cell. Cells closely associated in each plot are more likely to transcribe similar genes and might thus belong to the same cell type. Expression values and coordinates for each dot were obtained from the original study. The color scale indicates expression level for a particular gene ranging from 0 (minimum expression value observed in the dataset for that gene, usually corresponding to non detectable expression) to 100 (maximum expression value observed in the dataset for that gene). Expression of *FDCSP* is observed in a group of cells indicated by a black arrow in (A) well distinct from cells expressing prototypical B cell markers (B-D).

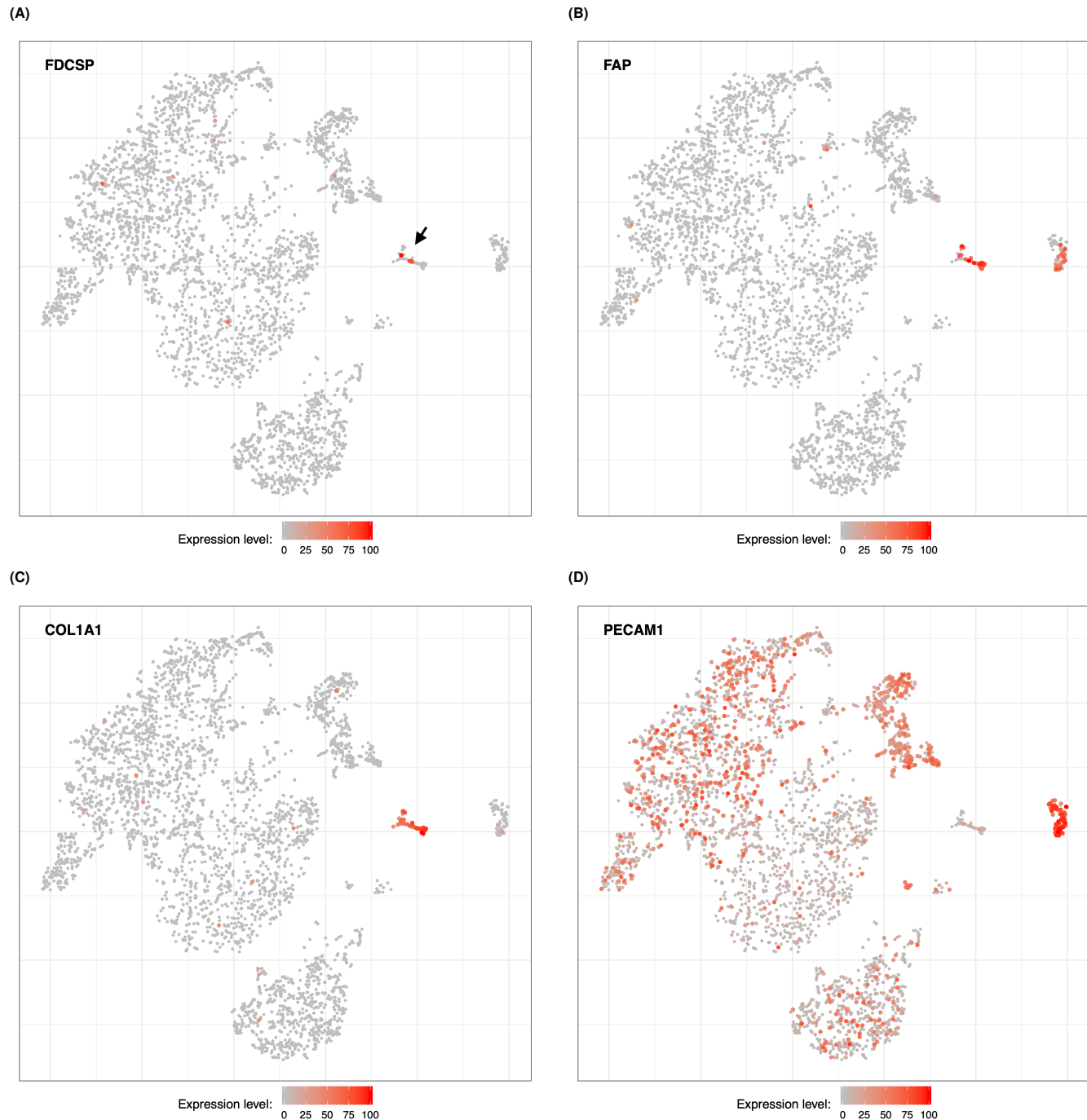


Fig. S6. | FDCSP is expressed in a subset of fibroblasts in melanoma. Two-dimensional visualizations (tSNE plots) of single-cell RNA sequencing data obtained from melanoma tumours and published in (27). Each dot represents the transcriptional profile of a single cell. Cells closely associated in each plot are more likely to transcribe similar genes and might thus belong to the same cell type. Expression values and coordinates for each dot were obtained from the original study. The color scale indicates expression level for a particular gene ranging from 0 (minimum expression value observed in the dataset for that gene, usually corresponding to non detectable expression) to 100 (maximum expression value observed in the dataset for that gene). **A.** Expression of *FDCSP*. The black arrow indicates a group of transcriptionally related cells containing *FDCSP*⁺ cells. **B.** Expression of *FAP*. **C.** Expression of *COL1A1*. **D.** Expression of *PECAM1/CD31*.

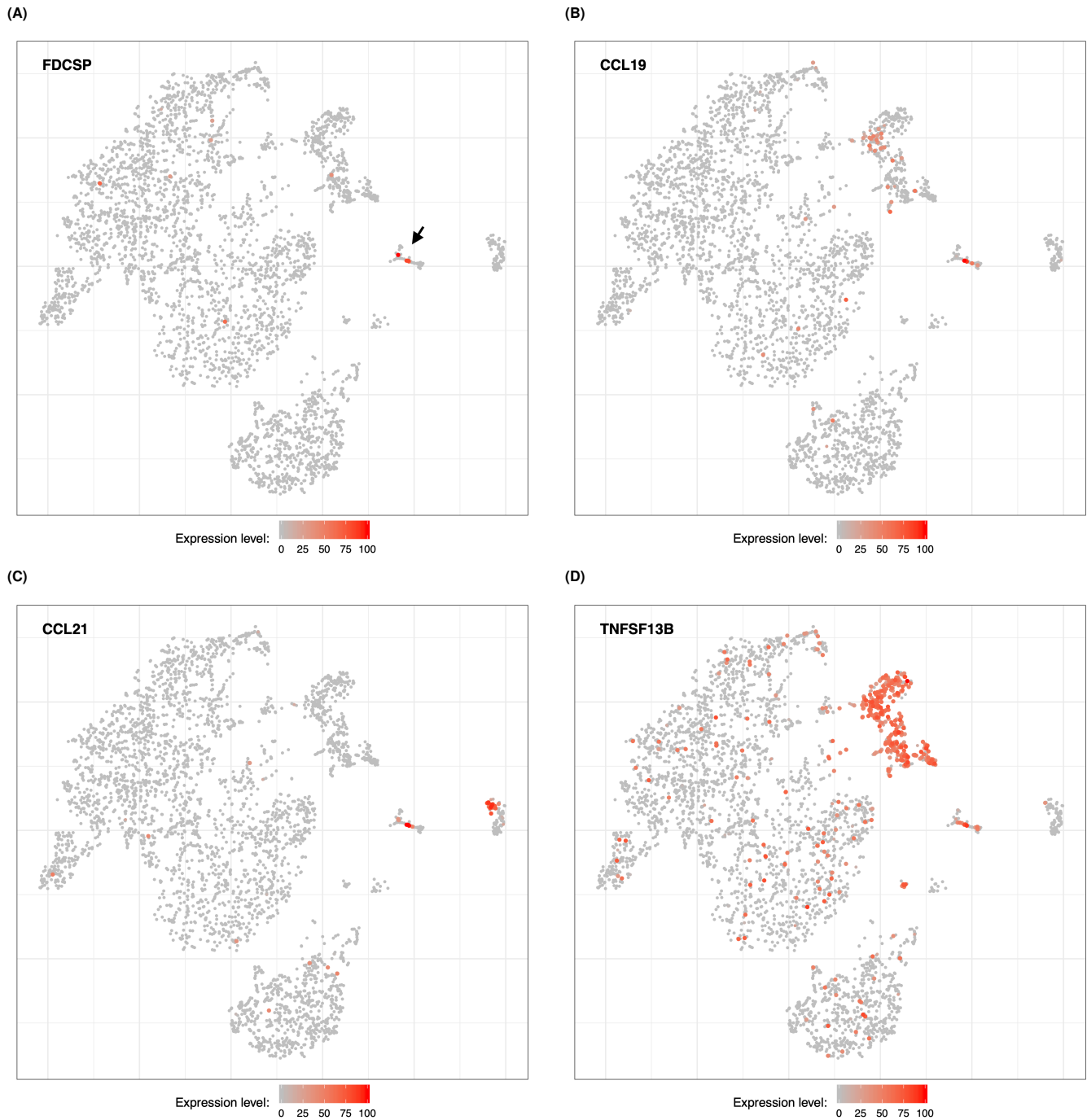


Fig. S7. | FDCSP+ cells express markers of FRCs in melanoma. Two-dimensional visualizations (tSNE plots) of single-cell RNA sequencing data obtained from melanoma tumours and published in (27). Each dot represents the transcriptional profile of a single cell. Cells closely associated in each plot are more likely to transcribe similar genes and might thus belong to the same cell type. Expression values and coordinates for each dot were obtained from the original study. The color scale indicates expression level for a particular gene ranging from 0 (minimum expression value observed in the dataset for that gene, usually corresponding to non detectable expression) to 100 (maximum expression value observed in the dataset for that gene). **A.** Expression of *FDCSP*. The black arrow indicates a group of transcriptionally related cells containing *FDCSP*+ cells. **B.** Expression of *CCL19*. **C.** Expression of *CCL21*. **D.** Expression of *TNFSF13B/BAFF*.

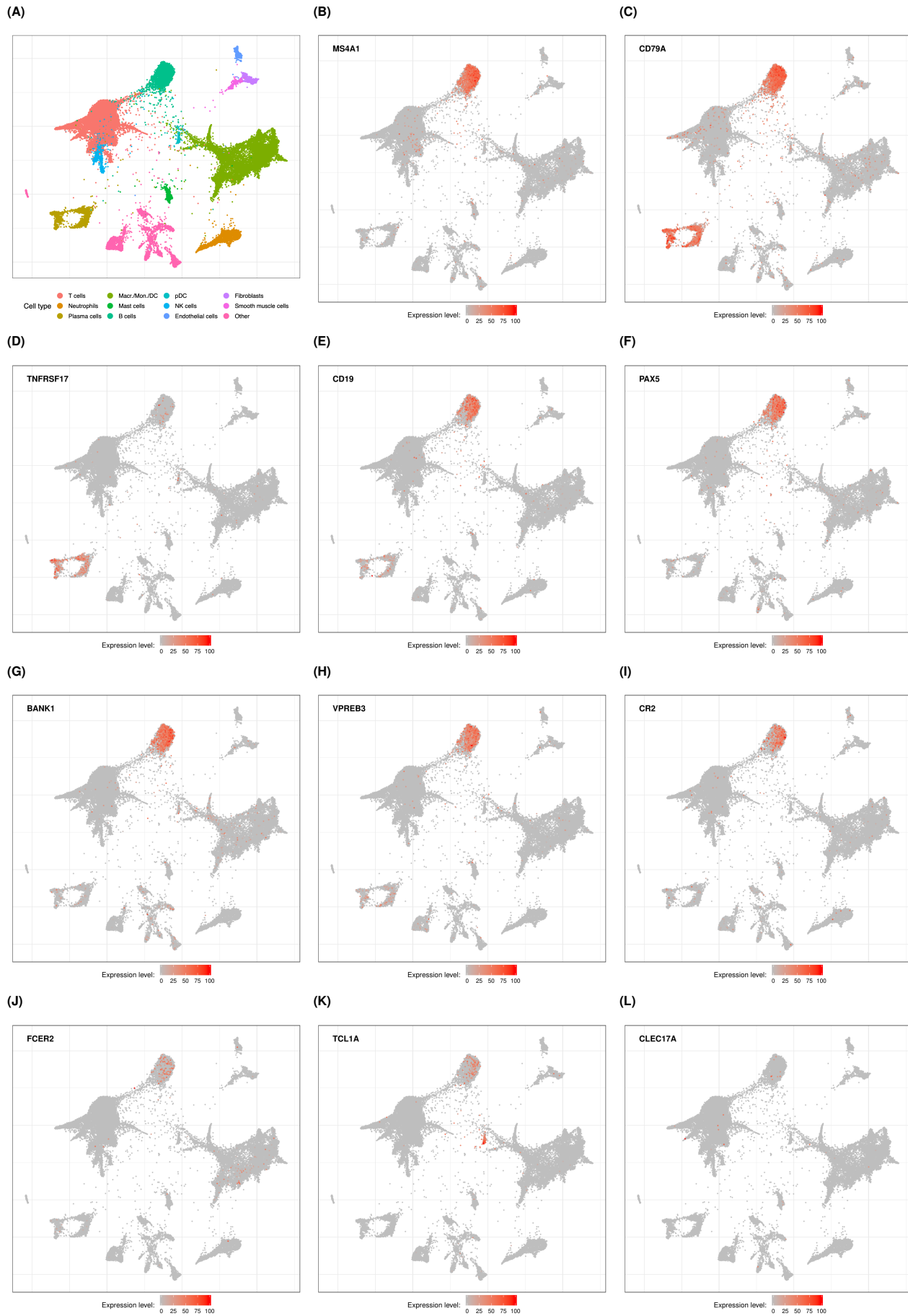


Fig. S8. | Expression of ICB response associated genes in single cells obtained from lung cancer tumours. Two-dimensional visualizations (SPRING plots) of single-cell RNA sequencing data obtained from lung cancer tumours and published in (25). Each dot represents the transcriptional profile of a single cell. Cells closely associated in each plot are more likely to transcribe similar genes and might thus belong to the same cell type. Expression values and coordinates for each dot were obtained from the original study. The expression level color scale indicates expression level for a particular gene ranging from 0 (minimum expression value observed in the dataset for that gene, usually corresponding to non detectable expression) to 100 (maximum expression value observed in the dataset for that gene). Panels B and C are included in the figure in order to further confirm the identity of cells annotated as "B cells" and "Plasma cells" in panel A. **A.** Cell types annotation as reported in the original study (25). **B.** Expression of *MS4A1/CD20*. **D.** Expression of *CD79A* is detectable in B cells and Plasma cells as expected. **D.** Expression of *TNFRSF17/BCMA* is detectable in Plasma cells but not in B cells as expected. **E.** Expression of *CD19*. **F.** Expression of *PAX5*. **G.** Expression of *BANK1*. **H.** Expression of *VPREB3*. **I.** Expression of *CR2*. **J.** Expression of *FCER2*. **K.** Expression of *TCL1A*, also detectable in Plasmacytoid dendritic cells (pDC, see panel A). **L.** Expression of *CLEC17A*.

322

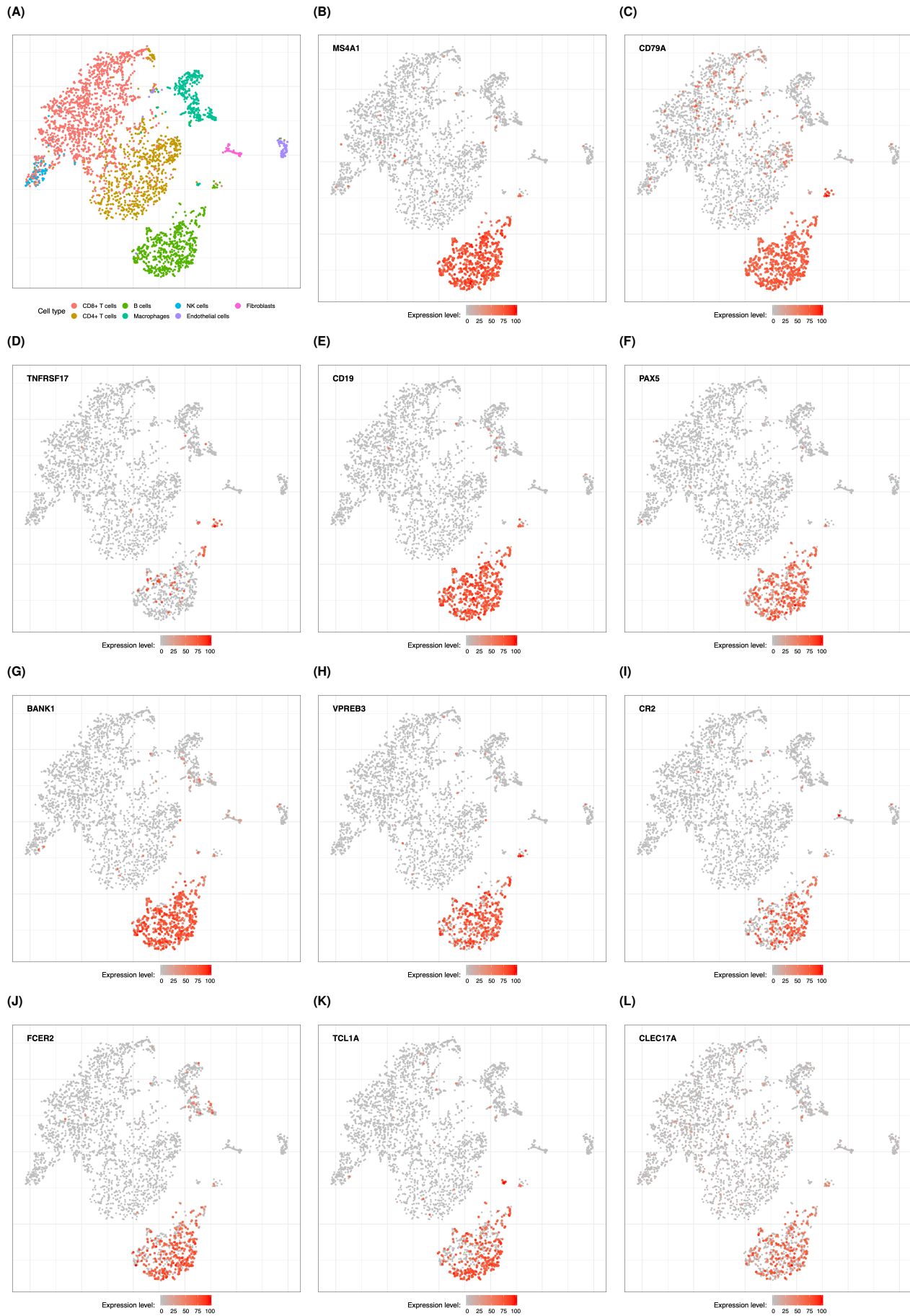


Fig. S9. | Expression of ICB response associated genes in single cells obtained from melanoma tumours. Two-dimensional visualizations (tSNE plots) of single-cell RNA sequencing data obtained from melanoma tumours and published in (27). Each dot represents the transcriptional profile of a single cell. Cells closely associated in each plot are more likely to transcribe similar genes and might thus belong to the same cell type. Expression values and coordinates for each dot were obtained from the original study. The expression level color scale indicates expression level for a particular gene ranging from 0 (minimum expression value observed in the dataset for that gene, usually corresponding to non detectable expression) to 100 (maximum expression value observed in the dataset for that gene). Panels B and C are included in the figure in order to further confirm the identity of cells annotated as "B cells" and "Plasma cells" in panel A. **A.** Cell types annotation as reported in the original study (27). **B.** Expression of *MS4A1/CD20*. **C.** Expression of *CD79A*. **D.** Expression of *TNFRSF17/BCMA*. A small cluster of Plasma cells might be visible but was not clearly annotated in this dataset (see panel A). **E.** Expression of *CD19*. **F.** Expression of *PAX5*. **G.** Expression of *BANK1*. **H.** Expression of *VPREB3*. **I.** Expression of *CR2*. **J.** Expression of *FCER2*. **K.** Expression of *TCL1A*. A small cluster of pDC might be visible but was not clearly annotated in this dataset (see panel A). **L.** Expression of *CLEC17A*.

323

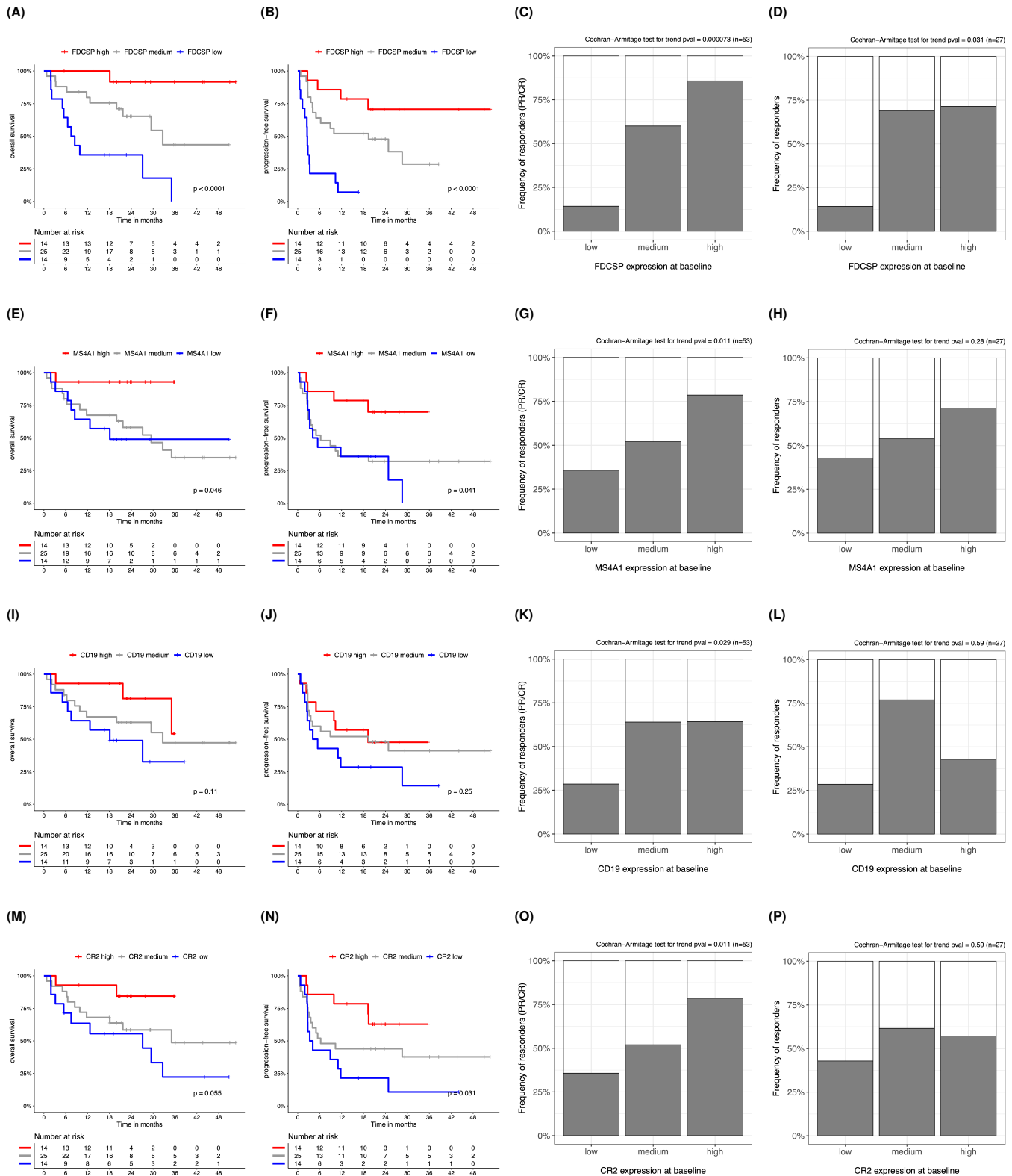


Fig. S10. | Predicting response in ICB treated patients using pre-treatment expression of FRCs or B cells markers.. A-B. Kaplan-Meier curves showing different overall survival and progression-free survival in melanoma patients after commencing treatment with ICB. Patients from (10) were stratified in three groups according to pre-treatment expression of *FDCSP*. C-D. Association between pre-treatment expression of *FDCSP* and subsequent ICB response in melanoma patients from (10; Panel C) and in clear cell renal cell carcinoma patients from (12; Panel D). Patients were stratified in three groups according to pre-treatment expression of *FDCSP* maintaining the same proportions used in panel A and D. E-H. Corresponding results obtained using pre-treatment expression of *MS4A1/CD20*. I-L. Corresponding results obtained using pre-treatment expression of *CD19*. M-P. Corresponding results obtained using pre-treatment expression of *CR2*.

324

325 **Appendix S3: supplementary tables**

Table S1 | Top 50 genes for which pre-treatment expression is associated with subsequent ICB response in melanoma. Genes are ordered by the column score which takes into account both p-value and $\log_2(fc)$: score = $\sqrt{-\log_{10}(p - \text{value}) * |\log_2(fc)| * \text{sign}(\log_2(fc))}$. The complete list is provided in a separate spreadsheet file (icb_resp_baseline.xlsx).

	gene	$\log_2(fc)$	$\log_2(fc)$ se	p-value	padj	stat	description	score
1	CR2	2.5	0.27	3.3E-21	4.9E-17	9.5	complement C3d receptor 2	7.1
2	FCER2	2.2	0.32	1.3E-13	6.3E-10	7.4	Fc fragment of IgE receptor II	5.3
3	CLEC17A	2	0.28	1.9E-14	1.5E-10	7.7	C-type lectin domain containing 17A	5.3
4	PAX5	2.2	0.33	8.2E-13	3.1E-09	7.2	paired box 5	5.1
5	FDCSP	2.2	0.36	6.7E-11	1.7E-07	6.5	follicular dendritic cell secreted protein	4.7
6	CD19	1.8	0.3	1.2E-11	3.5E-08	6.8	CD19 molecule	4.5
7	TCL1A	1.9	0.34	4.2E-10	6.3E-07	6.2	T cell leukemia/lymphoma 1A	4.2
8	VPREB3	1.7	0.31	1.7E-10	2.9E-07	6.4	V-set pre-B cell surrogate light chain 3	4.1
9	BANK1	1.6	0.28	1E-10	2E-07	6.5	B cell scaffold protein with ankyrin repeats 1	4
10	MS4A1	1.7	0.32	1.2E-09	1.6E-06	6.1	membrane spanning 4-domains A1	3.9
11	TLR10	1.4	0.24	9E-11	1.9E-07	6.5	toll like receptor 10	3.8
12	BLK	1.3	0.25	3.1E-09	3.6E-06	5.9	BLK proto-oncogene, Src family tyrosine kinase	3.3
13	MUC7	1.7	0.44	6.6E-07	0.00038	5	mucin 7, secreted	3.3
14	PSCA	1.5	0.31	4.1E-08	3.8E-05	5.5	prostate stem cell antigen	3.3
15	SPIB	1.3	0.26	9.9E-09	9.9E-06	5.7	Spi-B transcription factor	3.3
16	CYP4F11	1.4	0.31	5.1E-08	4.5E-05	5.4	cytochrome P450 family 4 subfamily F member 11	3.2
17	FAM129C	1.2	0.23	5.3E-09	5.7E-06	5.8	family with sequence similarity 129 member C	3.2
18	CNR2	1.2	0.25	6.6E-08	5.5E-05	5.4	cannabinoid receptor 2	2.9
19	CUX2	1.3	0.3	3.2E-07	0.0002	5.1	cut like homeobox 2	2.9
20	FCRL1	1.3	0.33	1E-06	0.00053	4.9	Fc receptor like 1	2.8
21	CCR7	1.2	0.25	2E-07	0.00014	5.2	C-C motif chemokine receptor 7	2.8
22	P2RX5	1.1	0.24	2.2E-07	0.00015	5.2	purinergic receptor P2X 5	2.7
23	GPX2	1.1	0.29	3E-06	0.0014	4.7	glutathione peroxidase 2	2.5
24	TSPAN8	1.2	0.38	1.1E-05	0.0035	4.4	tetraspanin 8	2.5
25	TNFRSF13C	0.98	0.22	8.7E-07	0.00048	4.9	TNF receptor superfamily member 13C	2.4
26	CCL21	1.2	0.39	1.6E-05	0.0048	4.3	C-C motif chemokine ligand 21	2.4
27	ABAT	0.9	0.21	1.2E-06	0.00061	4.9	4-aminobutyrate aminotransferase	2.3
28	RGS13	1.1	0.34	1.8E-05	0.0051	4.3	regulator of G protein signaling 13	2.2
29	GP1BA	0.88	0.21	2.1E-06	0.00096	4.7	glycoprotein Ib platelet subunit alpha	2.2
30	STAP1	1	0.31	1.4E-05	0.0044	4.3	signal transducing adaptor family member 1	2.2
31	CD79A	1	0.37	2.7E-05	0.0068	4.2	CD79a molecule	2.2
32	SLC27A2	1	0.32	1.8E-05	0.0051	4.3	solute carrier family 27 member 2	2.2
33	C4A	0.88	0.23	4.9E-06	0.002	4.6	complement C4A (Rodgers blood group)	2.2
34	TREML2	0.93	0.26	9.8E-06	0.0033	4.4	triggering receptor expressed on myeloid cells like 2	2.2
35	APOC4-APOC2	1.1	0.46	5.1E-05	0.011	4.1	APOC4-APOC2 readthrough (NMD candidate)	2.2
36	DNASE1L3	0.96	0.3	1.8E-05	0.0051	4.3	deoxyribonuclease 1 like 3	2.1
37	LRMP	0.78	0.2	5.5E-06	0.0021	4.5	lymphoid restricted membrane protein	2
38	AMDHD1	0.83	0.25	1.7E-05	0.0051	4.3	amidohydrolase domain containing 1	2
39	CPS1	0.88	0.31	3.5E-05	0.0085	4.1	carbamoyl-phosphate synthase 1	2
40	PLAC8	0.84	0.27	2.5E-05	0.0066	4.2	placenta associated 8	2
41	CCR6	0.96	0.46	9.7E-05	0.017	3.9	C-C motif chemokine receptor 6	2
42	SELL	0.8	0.25	2E-05	0.0054	4.3	selectin L	1.9
43	C4B	0.78	0.25	2.5E-05	0.0066	4.2	complement C4B (Chido blood group)	1.9
44	MUC3A	0.77	0.27	4.1E-05	0.0092	4.1	mucin 3A, cell surface associated	1.8
45	VIPR1	0.78	0.32	7.4E-05	0.014	4	vasoactive intestinal peptide receptor 1	1.8
46	IGHV1-58	0.89	0.62	0.00026	0.035	3.7	immunoglobulin heavy variable 1-58	1.8
47	SLC22A1	0.79	0.37	0.00011	0.018	3.9	solute carrier family 22 member 1	1.8
48	CFHR4	0.9	0.77	0.00036	0.039	3.6	complement factor H related 4	1.8
49	ABCG5	0.79	0.37	0.00012	0.019	3.9	ATP binding cassette subfamily G member 5	1.8
50	OIT3	0.83	0.47	0.00018	0.027	3.7	oncprotein induced transcript 3	1.8

Table S2 | Multiple linear regression analysis of ICB response. Expression values of cell type specific markers were summarised by calculating their geometric mean. The resulting summarised values were used as independent variables in a multiple linear regression model aimed at explaining ICB response. The table reports the regression coefficient estimates obtained by fitting the model to all pre-treatment melanoma samples available for this study (see Supplementary methods). The probability of observing estimates different from zero merely by chance was calculated by leveraging on the null distribution of the t-test statistic ($Pr(> |t|)$). The results show that expression of *FDCSP* is significantly associated with ICB response independently of genes expressed in major immune cell types. Asterisks indicate the level of statistical significance: *** indicates p-value ≤ 0.001 , ** indicates p-value ≤ 0.01 , * indicates p-value ≤ 0.05 .

	Cell type	Markers	Estimate	Std. Error	t value	Pr(> t)	
1	CD8+ T cells	CD8A, CD8B, TRAC	0.032	0.078	0.40	0.69	
2	CD4+ T cells	CD4, TRAC	0.057	0.110	0.52	0.60	
3	NK cells	GNLY, KLRF1	-0.089	0.092	-0.96	0.34	
4	B cells	MS4A1, CD19	0.044	0.049	0.90	0.37	
5	Macrophages	CD163, MARCO	-0.014	0.049	-0.29	0.77	
6	Dendritic cells	CD1A, CD1B, CD1E, LILRA4	-0.053	0.075	-0.70	0.48	
7	FDCSP+ cells	FDCSP	0.071	0.027	2.60	0.0092	**

Table S3 | Multiple linear regression analysis of ICB response, including plasma cell markers. expression of *FDCSP* is significantly associated with ICB response independently of genes expressed in major immune cell types, including Plasma cells. Asterisks indicate the level of statistical significance: *** indicates p-value ≤ 0.001 , ** indicates p-value ≤ 0.01 , * indicates p-value ≤ 0.05 .

	Cell type	Markers	Estimate	Std. Error	t value	Pr(> t)	
1	CD8+ T cells	CD8A, CD8B, TRAC	0.077	0.082	0.93	0.35	
2	CD4+ T cells	CD4, TRAC	0.049	0.110	0.45	0.65	
3	NK cells	GNLY, KLRF1	-0.074	0.092	-0.80	0.42	
4	B cells	MS4A1, CD19	0.078	0.053	1.50	0.14	
5	Macrophages	CD163, MARCO	-0.019	0.049	-0.40	0.69	
6	Dendritic cells	CD1A, CD1B, CD1E, LILRA4	-0.059	0.075	-0.78	0.44	
7	Plasma cells	TNFRSF17, MZB1	-0.093	0.056	-1.70	0.098	
8	FDCSP+ cells	FDCSP	0.067	0.027	2.50	0.014	*

Table S4 | Multiple linear regression analysis of ICB response, excluding *FDCSP*. Expression of B cell markers is significantly associated with ICB response independently of CD8+ T cells and other immune cell types. However, such association becomes statistically non-significant when expression of *FDCSP* is taken into account in the multiple regression model (Table S2 and Table S3). Asterisks indicate the level of statistical significance: *** indicates p-value ≤ 0.001 , ** indicates p-value ≤ 0.01 , * indicates p-value ≤ 0.05 .

	Cell type	Markers	Estimate	Std. Error	t value	Pr(> t)	
1	CD8+ T cells	CD8A, CD8B, TRAC	0.096	0.083	1.20	0.25	
2	CD4+ T cells	CD4, TRAC	0.044	0.110	0.40	0.69	
3	NK cells	GNLY, KLRF1	-0.045	0.093	-0.48	0.63	
4	B cells	MS4A1, CD19	0.120	0.051	2.20	0.027	*
5	Macrophages	CD163, MARCO	-0.018	0.049	-0.37	0.71	
6	Dendritic cells	CD1A, CD1B, CD1E, LILRA4	-0.073	0.076	-0.97	0.33	
7	Plasma cells	TNFRSF17, MZB1	-0.110	0.056	-1.90	0.064	

Table S5 | Top 50 genes up-regulated in FDCSP+ fibroblasts compared to FDCSP- fibroblasts detected by using single-cell RNAseq data. Differential gene expression analysis comparing single-cell transcriptomes of FDCSP+ fibroblasts versus FDCSP- fibroblasts obtained from lung cancer (NSCLC) and melanoma tumours (MEL). The analysis was performed using gene expression data published in (25, 27). Results from both datasets were meta-analysed using the RankProduct method (RP; see supplementary methods). The complete list is provided in a separate spreadsheet file (FDCSP_pos_vs_FDCSP_neg_fibroblasts.xlsx).

	gene	NSCLC_log ₂ (fc)	NSCLC_pvalue	MEL_log ₂ (fc)	MEL_pvalue	description	RP
1	CCL21	0.91	2.5E-16	12	8.5E-13	C-C motif chemokine ligand 21	1.4
2	FDCSP	1.7	3.2E-127	7.5	4.7E-17	follicular dendritic cell secreted protein	1.4
3	CCL19	1.2	7.2E-11	8.4	1.3E-08	C-C motif chemokine ligand 19	3.9
4	SLCO2B1	0.33	6.9E-10	2.9	2.3E-11	solute carrier organic anion transporter family member 2B1	10
5	TNFSF13B	0.71	7.5E-09	4.2	3.5E-06	TNF superfamily member 13b	11
6	CADM3	0.49	1.3E-15	2	9.1E-09	cell adhesion molecule 3	12
7	C3	1.8	7.3E-06	4.3	0.01	complement C3	18
8	C7	0.83	0.00043	4.7	0.00025	complement C7	19
9	CP	0.22	9E-07	3.4	2.2E-12	ceruloplasmin	20
10	UBD	0.06	2.4E-10	7	6.2E-13	ubiquitin D	25
11	ADH1B	0.48	0.0069	4.6	2.6E-06	alcohol dehydrogenase 1B (class I), beta polypeptide	32
12	PAPLN	0.51	3.3E-09	2	0.016	papilin, proteoglycan like sulfated glycoprotein	39
13	CXCL13	0.23	3.4E-06	2.4	2.3E-07	C-X-C motif chemokine ligand 13	41
14	VCAM1	0.56	0.0023	4	0.00055	vascular cell adhesion molecule 1	42
15	C10orf10	0.58	0.068	6.3	8.3E-05		42
16	CD74	0.37	0.036	6.5	7.5E-05	CD74 molecule	45
17	RBP5	0.18	4E-08	3.3	0.00011	retinol binding protein 5	46
18	CXCL14	0.77	0.0049	4.4	0.023	C-X-C motif chemokine ligand 14	54
19	PTGDS	0.25	0.22	8.9	2.8E-06	prostaglandin D2 synthase	60
20	DAAM1	0.38	0.0072	2.7	0.0001	dishevelled associated activator of morphogenesis 1	70
21	ZFP36L2	0.68	0.0014	2.1	0.014	ZFP36 ring finger protein like 2	71
22	NFIB	0.66	0.0018	1.9	0.0098	nuclear factor I B	73
23	CSF2RB	0.23	5.2E-06	1.7	3.2E-05	colony stimulating factor 2 receptor beta common subunit	74
24	RAMP3	0.02	0.043	6.4	4.7E-17	receptor activity modifying protein 3	76
25	CSMD1	0.2	0.0031	1.4	1.6E-10	CUB and Sushi multiple domains 1	79
26	IL6ST	0.54	0.022	2.6	0.001	interleukin 6 signal transducer	86
27	SLC22A3	0.04	0.0034	5.1	2.7E-08	solute carrier family 22 member 3	88
28	NFKBIA	0.45	0.1	4.7	0.0017	NFKB inhibitor alpha	88
29	C1R	0.89	0.0022	2.1	0.27	complement C1r	103
30	BIRC3	0.28	0.025	1.4	4.1E-08	baculoviral IAP repeat containing 3	105
31	SERPINB9	0.25	0.0011	3.6	0.016	serpin family B member 9	109
32	CTSH	0.08	0.08	6.4	3.6E-05	cathepsin H	110
33	IGFBP7	1.1	0.0097	1.6	0.18	insulin like growth factor binding protein 7	112
34	CTSS	0.39	5.5E-05	1.7	0.055	cathepsin S	114
35	CLK1	0.57	0.0013	1.7	0.068	CDC like kinase 1	120
36	ZBTB16	0.17	0.04	2.8	9.7E-06	zinc finger and BTB domain containing 16	120
37	RPL13	0.98	0.00015	0.35	0.24	ribosomal protein L13	124
38	LPAR1	0.31	0.00015	2.1	0.041	lysophosphatidic acid receptor 1	129
39	SOD2	0.62	0.12	3.5	0.014	superoxide dismutase 2	130
40	KLRK1	0.1	5.9E-10	0.97	0.00031	killer cell lectin like receptor K1	135
41	XIST	0.37	0.0089	2.1	0.013	X inactive specific transcript	136
42	IL33	0.29	1.3E-05	1.4	0.041	interleukin 33	138
43	IER3	0.51	0.032	2.5	0.027	immediate early response 3	139
44	HLA-DRB1	0.36	2.5E-06	1.3	0.21	major histocompatibility complex, class II, DR beta 1	139
45	CYP1B1	0.66	0.00034	1	0.23	cytochrome P450 family 1 subfamily B member 1	140
46	ARHGAP15	0.05	0.37	4	5.4E-10	Rho GTPase activating protein 15	144
47	JUN	0.92	0.026	1.9	0.17	Jun proto-oncogene, AP-1 transcription factor subunit	148
48	FKBP1A	0.36	0.05	2.1	0.0016	FKBP prolyl isomerase 1A	152
49	CLU	0.21	0.29	5.5	0.001	clusterin	154
50	IRF8	0.08	0.019	2.4	8.4E-07	interferon regulatory factor 8	154
51	CXCL12	0.26	0.12	3.6	0.0021	C-X-C motif chemokine ligand 12	158
52	C1S	0.58	0.068	2.7	0.054	complement C1s	158
53	TMEM176B	0.28	0.25	4.2	0.0017	transmembrane protein 176B	161
54	NAP1L1	0.69	0.0041	1.2	0.13	nucleosome assembly protein 1 like 1	164
55	ABHD2	0.6	2.3E-05	0.43	0.37	abhydrolase domain containing 2	168
56	KEL	0	0.88	3.3	9.4E-14	Kell metallo-endopeptidase (Kell blood group)	183
57	LAMA3	0.05	0.0031	2.1	1.4E-06	laminin subunit alpha 3	189
58	STRA6	0.08	0.038	1.6	6.2E-08	stimulated by retinoic acid 6	195
59	RBP1	0.07	0.25	4.6	0.00017	retinol binding protein 1	196
60	ABCC3	0.04	0.14	3.2	5.2E-07	ATP binding cassette subfamily C member 3	198

Table S6 | Top 50 genes down-regulated in FDCSP+ fibroblasts compared to FDCSP- fibroblasts detected by using single-cell RNAseq data. Differential gene expression analysis comparing single-cell transcriptomes of FDCSP+ fibroblasts versus FDCSP- fibroblasts obtained from lung cancer (NSCLC) and melanoma tumours (MEL). The analysis was performed using gene expression data published in (25, 27). Results from both datasets were meta-analysed using the RankProduct method (RP; see supplementary methods). The complete list is provided in a separate spreadsheet file (FDCSP_pos_vs_FDCSP_neg_fibroblasts.xlsx).

gene	NSCLC_log ₂ (fc)	NSCLC_pvalue	MEL_log ₂ (fc)	MEL_pvalue	description	RP	
1	FN1	-1.1	0.0024	-5.8	0.001	fibronectin 1	14226
2	CTHRC1	-0.79	0.0042	-4.9	0.0032	collagen triple helix repeat containing 1	14222
3	TIMP3	-0.87	0.019	-3.2	0.0017	TIMP metalloproteinase inhibitor 3	14218
4	COL1A2	-1.1	0.011	-3.1	0.0032	collagen type I alpha 2 chain	14212
5	COL1A1	-1.6	0.011	-3	0.0056	collagen type I alpha 1 chain	14210
6	COL5A1	-0.87	0.0061	-2.9	0.0053	collagen type V alpha 1 chain	14206
7	ARF4	-0.43	0.0095	-3.2	0.0077	ADP ribosylation factor 4	14204
8	LGALS1	-0.46	0.13	-5.8	0.00057	galectin 1	14203
9	COL5A2	-0.81	0.019	-2.9	0.0073	collagen type V alpha 2 chain	14199
10	PRSS23	-0.34	0.084	-3.8	0.0044	serine protease 23	14194
11	POSTN	-0.6	0.11	-3.6	0.021	periostin	14187
12	MMP2	-0.48	0.14	-3.1	0.011	matrix metalloproteinase 2	14180
13	COL8A1	-0.35	0.12	-3.3	0.0094	collagen type VIII alpha 1 chain	14176
14	VCAN	-0.42	0.12	-3.1	0.011	versican	14176
15	SPON2	-0.32	0.038	-2.8	0.011	spondin 2	14174
16	CYB5R3	-0.38	0.024	-2.5	0.014	cytochrome b5 reductase 3	14161
17	ACTB	-0.4	0.078	-2.2	0.0053	actin beta	14160
18	ITGB5	-0.37	0.0093	-2.2	0.0094	integrin subunit beta 5	14158
19	CAV1	-0.2	0.15	-3.9	0.0032	caveolin 1	14154
20	ITGA11	-0.3	0.035	-2.4	0.0094	integrin subunit alpha 11	14153
21	FBN1	-0.53	0.012	-2.4	0.015	fibrillin 1	14152
22	CHPF	-0.17	0.067	-2.7	0.0044	chondroitin polymerizing factor	14151
23	FKBP9	-0.27	0.087	-2.5	0.006	FKBP prolyl isomerase 9	14150
24	ECM1	-0.14	0.089	-3.4	0.0027	extracellular matrix protein 1	14145
25	ANXA5	-0.38	0.055	-2.1	0.0084	annexin A5	14145
26	LOX	-0.22	0.045	-3	0.023	lysyl oxidase	14137
27	RAB31	-0.45	0.033	-2.1	0.015	RAB31, member RAS oncogene family	14122
28	ITGB1	-0.69	0.017	-2.3	0.024	integrin subunit beta 1	14122
29	CNN2	-0.52	0.0089	-2	0.014	calponin 2	14116
30	TPM1	-0.29	0.12	-2.7	0.027	tropomyosin 1	14108
31	CTGF	-0.32	0.16	-3.2	0.05		14105
32	INHBA	-0.41	0.097	-2.3	0.024	inhibin subunit beta A	14102
33	S100A11	-0.23	0.34	-4.3	0.001	S100 calcium binding protein A11	14101
34	GNPMB	-0.14	0.16	-3.4	0.0032	glycoprotein nmb	14100
35	PXDN	-0.4	0.051	-2	0.016	peroxidase	14099
36	THBS2	-0.47	0.091	-2.6	0.044	thrombospondin 2	14098
37	SFRP2	-0.29	0.36	-4.1	0.043	secreted frizzled related protein 2	14096
38	CAPN2	-0.15	0.076	-2.6	0.021	calpain 2	14091
39	EFEMP2	-0.12	0.13	-3.8	0.0046	EGF containing fibulin extracellular matrix protein 2	14085
40	TPM4	-0.42	0.18	-2	0.014	tropomyosin 4	14083
41	COP9	-0.18	0.19	-2.4	0.014	COP9 signalosome subunit 8	14071
42	FHL2	-0.12	0.15	-2.8	0.0094	four and a half LIM domains 2	14065
43	CAPZB	-0.29	0.19	-1.9	0.013	capping actin protein of muscle Z-line subunit beta	14065
44	NOP10	-0.12	0.11	-2.7	0.019	NOP10 ribonucleoprotein	14062
45	CERCAM	-0.13	0.22	-3.5	0.0044	cerebral endothelial cell adhesion molecule	14061
46	FSCN1	-0.22	0.12	-1.6	0.0051	fascin actin-bundling protein 1	14057
47	NDUFB10	-0.12	0.12	-2.6	0.014	NADH:ubiquinone oxidoreductase subunit B10	14054
48	HSPG2	-0.23	0.065	-1.6	0.0098	heparan sulfate proteoglycan 2	14053
49	SULF1	-0.48	0.04	-2.2	0.052	sulfatase 1	14044
50	PLAT	-0.26	0.037	-1.9	0.027	plasminogen activator, tissue type	14042
51	SPARC	-1.1	0.0011	-1.8	0.033	secreted protein acidic and cysteine rich	14036
52	CD55	-0.15	0.11	-2.1	0.022	CD55 molecule (Cromer blood group)	14034
53	CALM2	-0.25	0.28	-2.5	0.044	calmodulin 2	14020
54	VDAC2	-0.14	0.15	-2.6	0.032	voltage dependent anion channel 2	14019
55	REXO2	-0.21	0.15	-2	0.029	RNA exonuclease 2	14019
56	HTRA1	-0.15	0.31	-2.9	0.0044	HtrA serine peptidase 1	14010
57	MFAP2	-0.13	0.22	-3.1	0.016	microfibril associated protein 2	14010
58	MFAP5	-0.12	0.22	-3.8	0.021	microfibril associated protein 5	14009
59	GSTP1	-0.19	0.27	-2.3	0.024	glutathione S-transferase pi 1	14004
60	ASPN	-0.33	0.076	-2.5	0.097	asporin	14002

Table S7 | Expression of FDCCSP is an independent predictor of response to immune checkpoint blockade. FDR values used to generate Fig. 1D

	TRAC	TRBC1	TRBC2	CD8A	GZMA	GZMB	PRFI	GNLY	KLRF1	NKG7	CCL5	IFNG	CXCL9	CXCL10	CXCL11	IDO1	CLEC9A	XCR1	MS4A1	CD19	PAX5	BANK1	FDCCSP	
FCER2	1.5E-02	1.6E-05	5.0E-04	7.6E-08	1.2E-07	3.3E-05	3.0E-05	7.3E-02	1.3E-03	1.4E-05	1.1E-08	4.3E-10	1.1E-08	5.4E-11	9.9E-12	1.5E-06	2.7E-05	1.8E-06	1.0E+00	1.0E+00	1.0E+00	1.0E+00	1.0E+00	3.5E-01
TCL1A	3.0E-01	1.3E-01	5.1E-01	5.3E-02	4.7E-04	3.3E-03	1.6E-03	1.2E-01	1.8E-03	9.4E-03	1.9E-04	4.3E-03	7.8E-03	2.9E-05	3.6E-07	3.9E-02	1.0E-02	4.1E-04	5.5E-01	1.0E+00	1.0E+00	1.0E+00	1.0E+00	1.0E+00
VPREB3	2.0E-01	3.2E-01	1.9E-01	5.1E-04	1.1E-05	2.8E-03	1.9E-04	5.4E-02	1.5E-03	7.8E-04	1.8E-05	6.6E-05	8.1E-05	6.9E-07	1.6E-08	7.4E-03	1.3E-02	2.3E-04	9.3E-02	1.0E+00	1.0E+00	1.0E+00	1.0E+00	1.0E+00
PAX5	8.4E-01	6.1E-01	5.0E-01	3.5E-02	7.5E-04	4.3E-03	1.0E-02	1.7E-01	3.6E-03	1.7E-02	2.0E-04	8.2E-05	1.9E-04	2.0E-07	2.2E-09	1.9E-02	1.9E-02	1.8E-03	1.0E+00	1.0E+00	1.0E+00	1.0E+00	1.0E+00	1.0E+00
CLEC17A	1.5E-03	1.1E-03	1.3E-03	1.4E-05	5.6E-07	2.6E-04	2.9E-05	1.5E-03	3.9E-05	9.7E-05	5.4E-07	8.1E-07	1.6E-06	3.7E-10	4.9E-12	6.7E-04	3.9E-05	2.2E-06	5.6E-01	4.7E-01	8.3E-01	1.9E-01	3.2E-01	3.3E-01
CR2	3.7E-07	2.0E-06	1.4E-06	5.0E-09	1.4E-11	1.4E-10	4.0E-09	1.1E-04	6.6E-06	3.6E-08	4.5E-13	1.7E-13	6.9E-14	3.7E-17	1.0E-18	3.4E-09	1.9E-04	4.7E-12	5.4E-01	7.8E-01	3.3E-01	5.3E-02	3.3E-01	3.3E-01
MS4A1	4.0E-04	3.5E-04	4.7E-04	2.1E-06	1.1E-08	1.0E-03	4.1E-04	8.2E-03	5.7E-03	1.1E-04	2.8E-08	1.1E-07	3.7E-07	9.0E-10	4.7E-12	1.9E-02	8.1E-02	1.2E-05	1.0E+00	1.0E+00	1.0E+00	1.0E+00	1.0E+00	1.0E+00
CD19	5.3E-02	5.4E-02	1.0E-01	2.6E-04	1.8E-06	1.0E-03	5.3E-04	2.8E-01	2.9E-04	4.7E-04	2.2E-06	9.1E-07	1.3E-06	1.9E-09	4.9E-12	1.0E-03	1.5E-03	2.1E-04	1.0E+00	1.0E+00	1.0E+00	1.0E+00	1.0E+00	1.0E+00
BANK1	1.4E-01	1.1E-01	1.8E-01	7.0E-04	2.1E-05	7.8E-03	5.5E-03	7.5E-01	1.5E-02	8.4E-03	2.4E-05	4.4E-06	1.3E-05	3.7E-08	6.2E-10	1.5E-02	5.4E-02	1.5E-04	1.0E+00	1.0E+00	1.0E+00	1.0E+00	1.0E+00	1.0E+00
FDCCSP	6.1E-05	2.5E-06	1.4E-05	1.2E-06	5.4E-09	1.1E-04	2.0E-07	3.6E-07	8.1E-07	9.6E-07	3.7E-07	4.0E-06	9.5E-07	1.1E-08	6.6E-10	1.6E-03	4.8E-04	3.9E-05	0.0E+00	1.8E-03	5.6E-03	5.3E-04	1.0E+00	1.0E+00